Defect and Diffusion Forum
ISSN: 1662-9507, Vol. 451, pp 63-73
doi:10.4028/p-ZlRu4c

Submitted: 2026-01-10
Revised: 2026-03-03
Accepted: 2026-03-04
Online: 2026-04-17

Thermal Crystallization Kinetics of PET, RPET and PEF for Sustainable Packaging

Evan Gargadennec[1,a], Yun-Mei Luo[1,b*], Eric Monteiro[2,c] and Luc Chevalier[1,d]

[1]Université Gustave Eiffel, MSME UMR 8208 CNRS, 5 bd Descartes, 77454 Marne-la-Vallée, France

[2]Laboratoire PIMM, Arts et Métiers Institute of Technology, CNRS, CNAM,151 boulevard de l'Hôpital, 75013 Paris, France

[a]evan.gargadennec2@univ-eiffel.fr, [b]yun-mei.luo@univ-eiffel.fr, [c]eric.monteiro@ensam.eu, [d]luc.chevalier@univ-eiffel.fr

Keywords: PEF, PET, RPET, Thermal analysis, DSC, DMA, Crystallization kinetics

Abstract. Poly(ethylene 2,5-furandicarboxylate) (PEF) is a bio-based polyester that is the subject of growing interest as a potential alternative to Poly(ethylene terephthalate) (PET) for sustainable packaging. Its excellent gas-barrier properties and reduced carbon footprint make it a promising candidate, but its use at industrial scale requires a solid understanding of how temperature and thermal history affect its mechanical and viscoelastic behavior. In this study, Differential Scanning Calorimetry (DSC), Dynamic Mechanical Thermal Analysis (DMA), and optical microscopy were used to characterize the thermal transitions and crystallization behavior of PEF, compared with PET and recycled PET (rPET). DSC results show that thermal crystallization of PEF proceeds very slowly, a result confirmed by in-situ microscopy. DMA measurements provide complementary information on the evolution of both storage and loss moduli with temperature, highlighting its dependence on crystallinity and thermal history. Together, these thermal and mechanical analyses clarify how PEF's crystallization behavior affects its thermo-mechanical response. From a processing perspective, the very slow thermal crystallization of PEF is advantageous for stretch blow molding (SBM) process of bottles, as the polymer remains essentially amorphous during heating and crystallizes predominantly under deformation during the fast forming stage.

1 Introduction

Poly(ethylene 2,5-furandicarboxylate) (PEF) has gained considerable attention as a bio-based polyester that could serve as a viable alternative to conventional poly(ethylene terephthalate) (PET) in packaging. Its combination of excellent gas-barrier properties [1], renewable sourcing [2] and lower environmental footprint has made it an appealing candidate for next-generation, sustainable packaging materials. Recent studies have explored various aspects of PEF's potential: Luan et al. [1] demonstrated its superior gas barrier properties combined with rapid degradation; Loos et al. [2] provided a comprehensive review of PEF synthesis, structure-property relationships, and end-of-life options; Forestier et al. [3] investigated its microstructural development upon stretching, revealing enhanced strain-induced crystallization behavior; Lightfoot et al. [4] used molecular modeling to explain the mechanism of oxygen diffusion in PEF compared to PET; Poulopoulou et al. [5] examined sustainable blends of PEF with other biobased polyesters; and Sousa et al. [6] proposed recommendations for replacing PET with biobased counterparts including PEF in packaging, fiber, and film applications. However, for applications such as bottle production or thermoforming [7,8], it remains essential to understand how PEF behaves during typical thermal cycles and how its structure develops compared with PET and recycled PET (rPET), which together dominate today's packaging market.

Although several studies [9-11] have examined the intrinsic properties of PEF, its crystallization behavior and its viscoelastic response under heating are still not fully understood. In particular, the slow crystallization kinetics often reported for PEF [12,13] may have important consequences for

industrial processes such as stretch blow molding (SBM) [14], where crystallization develops mainly under deformation. A direct comparison with PET and rPET is therefore essential to assess both the advantages and the limitations linked to the use of PEF in existing processing lines. For PET, it is well established that the SBM process leads to a marked increase in mechanical performance, as the material transitions from an amorphous preform to a semi-crystalline bottle [15]. In practice, crystallization induced by heating and by deformation occur simultaneously, and thermal crystallization is extremely fast [16]. This combination makes both simulation and experimental analysis particularly challenging.

In this study, the thermal behavior of PEF is examined and directly compared with that of PET and rPET using injection-molded plates as starting materials. These plates correspond to the material state before the SBM process, allowing a clearer understanding of how PEF responds to temperature and how its crystallization develops under controlled thermal conditions.

To investigate these aspects, three complementary experimental techniques were used. Differential Scanning Calorimetry (DSC) was first carried out to characterize the main thermal transitions and to estimate the degree of crystallinity under controlled heating rates. These measurements enable to follow the onset of crystallization and to compare the evolution of thermal behavior between PEF, PET and rPET. In parallel, optical microscopy was used to directly observe the development of crystalline structures during heating. This approach provides qualitative but valuable information on the kinetics and the morphology of crystallization and confirms that the transitions detected by DSC correspond to actual structural changes in the material. Finally, Dynamic Mechanical Thermal Analysis (DMA) was performed to follow the temperature dependence of the storage and loss moduli. The response obtained by DMA offers additional information on the influence of crystallinity and thermal history on the mechanical behavior of the three materials.

Taken together, these techniques provide a coherent basis for comparing the thermal and thermo-mechanical behavior of PEF with that of PET and rPET and help clarify the characteristics that may influence the processing of PEF in packaging applications.

2 Material and Methods

2.1 Materials and Sample Preparation

The virgin PET material used is RAMAPET N180, supplied by Sidel Group, France. Its glass transition temperature (T_g) is 78±2°C and its intrinsic viscosity is 0.80±0.02 dl/g. The bulk density of N180 is 830±30 kg/m^3. The recycled PET, referenced as MOPET, also supplied by Sidel Group, France, has an intrinsic viscosity of 0.85±0.02 dl/g and a bulk density of 900±50 kg/m^3. PEF material used for comparison is a bio-based polyester produced from FDCA monomers, supplied by Zhengzhou Alfa Chemical Co., Ltd, China. Its intrinsic viscosity falls within 0.63–0.85 dl/g, and the bulk density is approximately 1.38 g/cm³. All detailed specifications provided by the suppliers, including thermal, rheological, and optical properties for PET, rPET, and PEF granules, are summarized in the tables of the Appendix.

The PET, rPET and PEF granules were processed at the PIMM laboratory using an injection molding machine (DK Codim 175). Each material was dried prior to injection and then fed into the heating cylinder, where it was melted, homogenized and injected into a steel mold under controlled pressure and temperature conditions. The overall injection cycle was adjusted for each polymer in order to account for their specific thermal behavior, particularly the higher melting temperature of PET and the slower crystallization kinetics of PEF. Using these conditions, plates with dimensions 125 mm × 125 mm × 2.5 mm were produced for subsequent characterization (Fig.1).


(a)

(b)

Fig.1. (a) polymer granules; (b) injected plate

The injection conditions used for virgin PET, rPET and PEF are listed in Table 1. They include injection speed, injection and holding pressures, injection time, cooling time and mold temperature. PET and rPET were processed under similar conditions, with a slightly higher holding pressure for the recycled grade. Because of its distinct melting temperature, viscosity and crystallization behavior, PEF required lower temperature settings and a reduced injection speed to avoid degradation and to keep a stable melt flow. The processing parameters for PEF were selected based on its specific thermal and rheological properties reported in the literature. The lower injection melt temperature (225°C) was chosen because PEF has a lower melting point (205-215°C) compared to PET (245-255°C), and processing at temperatures suitable for PET would cause thermal degradation [13]. The reduced injection speed (40 mm/s) was necessary due to PEF's slower crystallization kinetics, which requires controlled flow to prevent premature solidification [3]. The higher mold temperature (40°C) accommodates PEF's higher glass transition temperature (86-90°C) to optimize cooling and part quality [12]. Additionally, the lower injection pressure (1050 bar) is justified by PEF's lower melt viscosity compared to PET at processing temperatures [12], while the higher holding pressure (700 bar) compensates for its different crystallization behavior to ensure proper packing [3]. These settings were validated through preliminary trials to ensure stable processing without degradation.

Table 1. Injection conditions for PET, rPET and PEF

Parameters	Virgin PET	Recycled PET	PEF
Injection speed	70 mm/s	70 mm/s	40 mm/s
Injection pressure	1150 bar	1200 bar	1050 bar
Holding pressure	500 bar	600 bar	700 bar
Holding time	6 s	6 s	6 s
Injection time	1.2 s	1.2 s	1.9 s
Cooling time	50 s	50 s	40 s
Mold temperature	20 °C	20 °C	40 °C
Injection melt temperature	255 °C	255 °C	225 °C

2.2 Differential Scanning Calorimetry (DSC) analysis

PEF, PET and rPET samples used for DSC analysis were cut from plates produced by injection molding.

2.2.1 Non-isothermal DSC measurements

DSC measurements were carried out to evaluate the thermal transitions and crystallization behavior of PET, rPET and PEF. The experimental protocol consisted of a heating cycle from 30 °C to 300 °C at 10 °C·min^{-1} followed by a cooling cycle from 300 °C back to 30 °C at the same rate.

2.2.2 Isothermal crystallization measurements

To investigate the crystallization kinetics in more detail, isothermal DSC experiments were carried out at selected temperatures with the protocol:

1. Heating cycle: 30°C to 250°C at 20°C.min-1
2. Isotherm: 250°C during 3 min
3. Cooling cycle: 250°C to the selected crystallization temperature at 100°C.min^{-1}

4. Isotherm at the selected crystallization temperature during 180 min
5. Cooling cycle: from the selected crystallization temperature to 40°C at 10°C.min-1
6. Heating cycle: 40°C to 250°C at 5°C.min-1

After melting, the samples were rapidly cooled (100°C·min^{-1}) to the target isothermal temperature using liquid nitrogen assistance.

In addition, the degree of crystallinity X_c can be determined directly from the DSC curve by analyzing the areas associated with melting and crystallization.

$$X_c = \frac{\Delta H_m - \Delta H_c}{\Delta H_{m0}} \quad (1)$$

where ΔH_m is the enthalpy absorbed during melting, ΔH_c the enthalpy released during cold crystallization and ΔH_{m0} the enthalpy of fusion of a fully crystalline material. According to [12], ΔH_{m0} is equal to 140 J·g^{-1} for both PET and PEF. This approach provides a way to quantify and compare the crystallinity of materials processed under different conditions, such as injection molding or SBM process.

2.3 Optical Microscopy: Isothermal Crystallization Observation

To further support the conclusions from the DSC analysis, optical microscopy was used to directly observe the crystallization behavior of PET and PEF. The objective of this experiment was to visualize, in real time, the evolution of crystalline structures under isothermal conditions and to confirm the much slower crystallization kinetics of PEF compared with PET.

Thin lamellae, with thickness of approximately 5 μm, were cut directly from the injection-molded plates of PET and PEF. Each specimen was placed on a temperature-controlled heating stage positioned under the microscope. The following thermal protocol was applied:

1. Heating from 30°C to 250°C.
2. Isothermal hold at 250°C for 5 min to ensure complete melting.
3. Rapid cooling from 250°C to the selected crystallization temperature T_i at 100°C·min^{-1}.
4. Isothermal crystallization at T_i for a duration t.

Microscopy images were recorded continuously throughout the isothermal stage to monitor the nucleation and growth of spherulites. By analyzing the time required for the crystalline domains of each polymer, it is possible to compare their crystallization kinetics.

2.4 Dynamic Mechanical Analysis (DMA): Method and experimental procedure

Dynamic Mechanical Analysis (DMA) was conducted to characterize the viscoelastic behavior of rPET and PEF as a function of temperature. Tests were performed using TA Instruments Q800 DMA devices at PIMM laboratory. Specimens measuring 40 × 12 × 2.5 mm³ were cut from the injection-molded plates and tested in single-cantilever mode. Firstly, a strain-sweep test was carried out to identify the linear viscoelastic region (LVR) for each material. This preliminary step ensures that all tests are performed at a strain amplitude low enough for the modulus to remain independent of deformation. Once the LVR was established, a temperature-ramp experiment was conducted at a constant oscillation frequency and at a constant oscillation strain amplitude selected inside the LVR. During these tests, the DMA system continuously recorded the evolution of E'. All tests were carried out under air atmosphere to mimic process conditions.

3 Results and Discussion

3.1 Thermal properties from DSC

3.1.1 Non-isothermal crystallization behavior

Figure 2 shows the DSC heating curves obtained for PET and PEF using the same experimental protocol explained in section. Under these identical conditions, PET exhibits the classical thermal signature of a semi-crystalline polymer: a well-defined glass transition around 78 °C, followed by a pronounced exothermic crystallization peak T_c corresponding to cold crystallization, and finally a

sharp endothermic melting peak T_m. In contrast, the PEF thermogram shows only the glass transition, with no detectable crystallization peak and no melting endotherm during the first heating. This difference means that, unlike PET, PEF does not crystallize under standard non-isothermal DSC conditions. The absence of both T_c and T_m indicates that PEF remains essentially amorphous throughout the entire heating ramp, confirming its slow thermal crystallization kinetics.

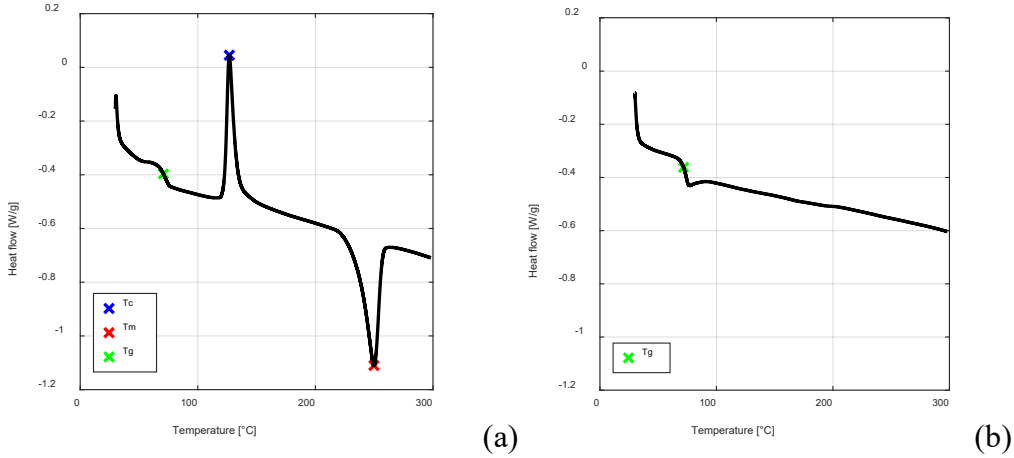

Fig. 2. Non-isothermal DSC test for (a) PET and (b) PEF

3.1.2 Thermal transition temperature

Table 2 summarizes the thermal transition parameters obtained from multiple DSC measurements. The mean T_g of PET is 71 °C, while rPET exhibits a very similar T_g of 71.8 °C with slightly reduced dispersion. These results confirm that mechanical recycling has no effect on the amorphous phase mobility. For PEF, the T_g is 72.9 °C, slightly higher than PET, consistent with the stronger intermolecular interactions associated with furanic rings.

The crystallization temperatures Tc ≈ 127.3 °C for PET and 130.0 °C for rPET. The higher T_c of rPET may arise from increased heterogeneity and residual nucleating species introduced during mechanical recycling. In contrast, no crystallization peak appears for PEF during cooling. This absence confirms that PEF crystallizes much more slowly than PET. As a result, the injected PEF plates are fully amorphous ($X_c \approx 0$). The PET and rPET plates obtained by injection show a measurable degree of crystallinity from Eq. 1, with X_c of approximately 9%.

The melting temperatures T_m for PET and rPET are highly consistent across samples, with mean values of 250.3 °C (PET) and 248.9 °C (rPET). For PEF, however, T_m cannot be measured from a simple heating because standard cooling produces no crystallization. Instead, melting temperatures must be obtained from isothermal crystallization experiments, as described in the following.

Table 2. Mean transition temperatures and dispersions measured by DSC

Material	T_g (°C)	T_c (°C)	T_m (°C)
PET	71.0 ± 0.6	127.4 ± 0.6	250.4 ± 0.7
rPET	71.6 ± 0.4	130.0 ± 0.9	248.7 ± 0.6
PEF	72.9 ± 0.7		

3.1.3 Isothermal crystallization behavior

The behavior of PET is shown in Fig. 3a. At temperatures close to its optimal crystallization range (around 150 °C), PET begins to crystallize almost immediately, often even before the temperature has stabilized at the isothermal plateau. This confirms the extremely fast crystallization kinetics reported in the literature [16]. Such rapid crystallization makes PET highly sensitive to the cooling rate during processing, because even small variations in temperature can significantly alter the final crystalline morphology.

In contrast, no crystallization peak is detected for PEF during an isothermal hold at 160 °C for 180 min (Fig. 3b). The absence of an exothermic signal indicates that the crystallization rate of PEF at

this temperature is extremely slow, remaining below the detection limit of conventional DSC. However, the appearance of a melting endotherm during the subsequent heating cycle demonstrates that a small amount of crystallization has occurred during the long isothermal stage, even though the crystallization peak itself could not be resolved. This confirms that PEF crystallizes during isothermal holds, but the process is too slow to be captured under standard DSC sensitivity, in contrast with the rapid crystallization exhibited by PET.

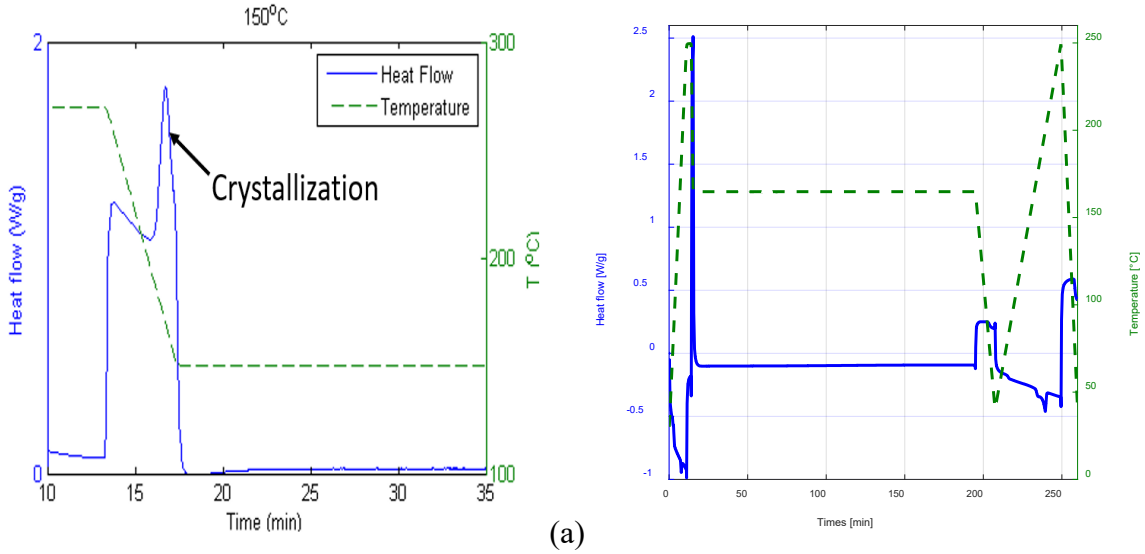

(a) (b)

Fig. 3. Isothermal crystallization measurements: (a) PET, showing very fast crystallization [16]; (b) PEF, with no detectable crystallization peak during the isothermal stage.

3.1.4 Quantitative analysis of PEF isothermal crystallization

To characterize PEF crystallization more precisely, isothermal DSC tests were performed. There is no crystallization peak that appears during the isothermal plateau, but a melting peak is observed during reheating. This indicates that crystallization does occur during the isotherm, but too slowly and with too low enthalpy to be detected directly as an exotherm. The degree of crystallinity X_c was therefore computed from the melting enthalpy:

$$X_c = \frac{\Delta H_m}{\Delta H_{m0}} \tag{2}$$

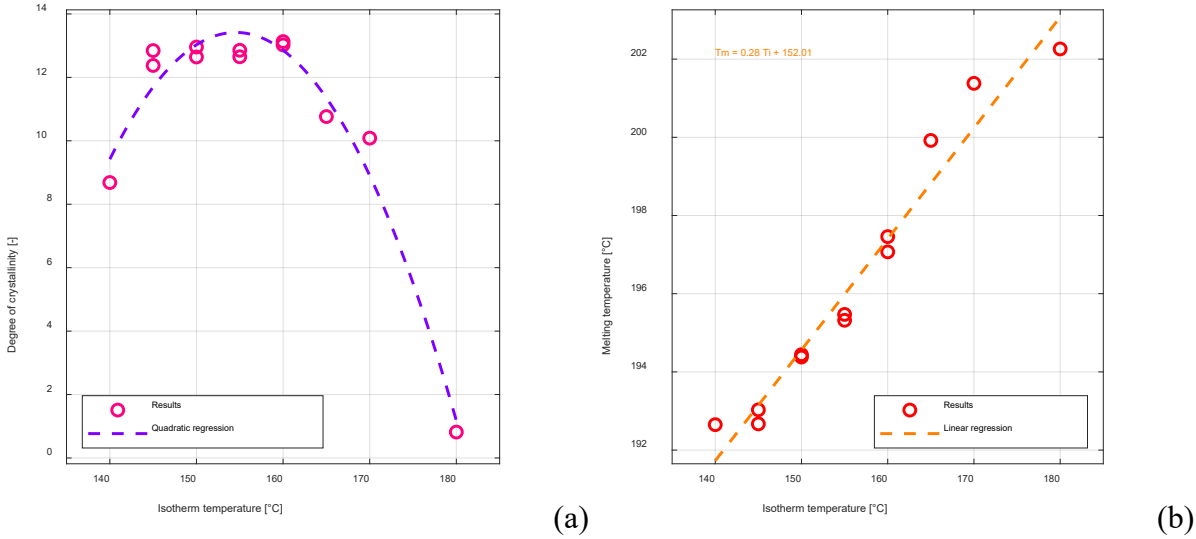

(a) (b)

Fig. 4. (a) Evolution of degree of crystallinity as a function of isothermal temperature; (b) Evolution of melting temperature as a function of isothermal temperature

The evolution of X_c as a function of T_i (Fig. 4a) shows that crystallinity reaches its maximum for 145 °C ≤ T_i ≤ 160 °C, identifying this range as the optimal crystallization temperature window of PEF. These temperatures are markedly lower than the PET T_c extracted from cooling scans, again confirming the slow kinetics and different thermodynamic behavior of PEF.
The melting temperature measured after each isothermal step increases approximately linearly with T_i (Fig. 4b). This behavior reflects the dependence of lamellar thickness on crystallization temperature, as described by the Gibbs–Thomson relation [17]:

$$T_m = T_{m0}\left(1 - \frac{2\,\sigma_e}{\Delta H_m\, L}\right) \quad (3)$$

where σ_e stands for the surface free energy of the lamella, L the lamellar thickness, T_{m0} the melting temperature of an ideal crystal of infinite size. Extrapolating the linear fit following a Hoffman Weeks approach [18] provides an estimate of the melting temperature of an ideal infinite crystal, $T_{m0} \approx 211$ °C.

3.2 Crystallization behavior from optical microscopy

Optical microscopy was used to provide a direct comparison of the crystallization behavior of PET and PEF under isothermal conditions. Thin sections of each material were heated above their melting temperature, rapidly cooled to the chosen isotherm, and observed in real time on a hot stage. For PET, crystallization occurred very rapidly even before the sample reached the isothermal temperature.

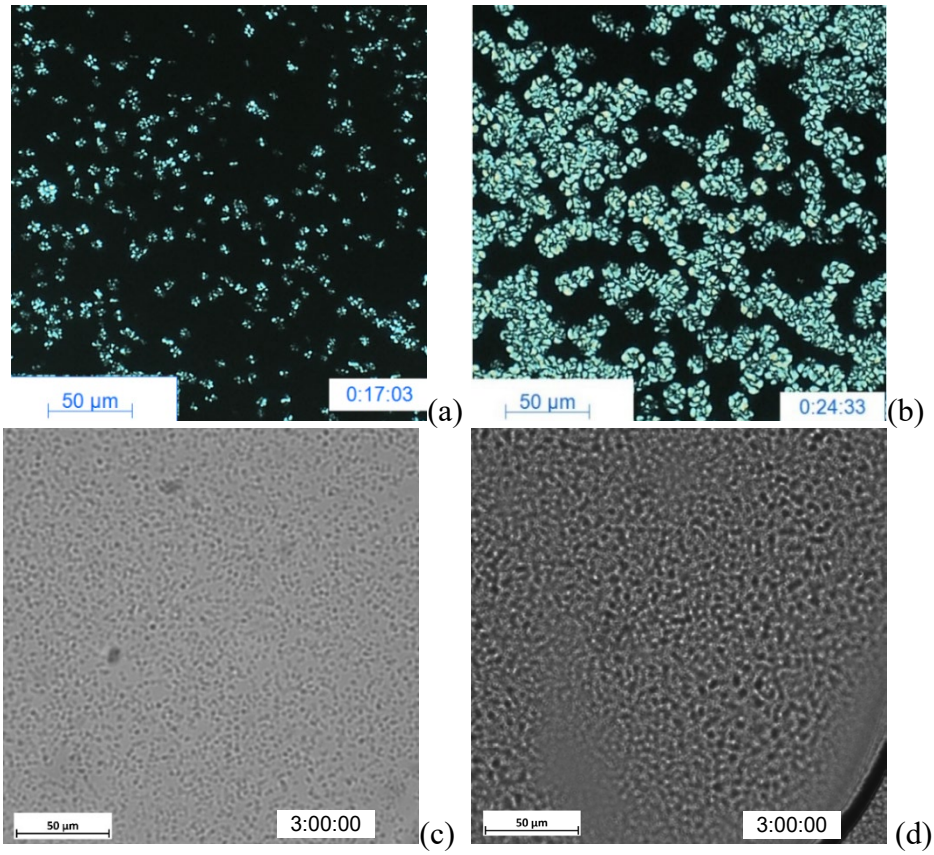

Fig. 5. Optical microscopy images of PEF and PET spherulite development during isothermal crystallization. (a) PET at 230 °C after 17 min; (b) PET at 230 °C after 24 min [16]; (c) PEF at 180 °C after 180 min; (d) PEF at 160 °C after 180 min

Figure 5 shows that at 230 °C, the first spherulites were present after about seventeen minutes, and by twenty-four minutes the microstructure was almost fully crystallized, with spherulites filling the field of view. For temperatures below 210 °C, crystallization occurs and completes too quickly to follow its evolution. This rapid development is consistent with the DSC results, confirming its high kinetic activity and strong sensitivity to cooling conditions. In contrast, Fig. 5 shows that for PEF, very few crystalline structures were observed at 180 °C even after 180 min, and a higher spherulite

density is observed at 160 °C compared with 180 °C after 180 min, but their growth is too slow to follow the evolution in real time.

3.3 Viscoelastic behavior from DMA

Dynamic Mechanical Analysis was carried out to examine how rPET and PEF respond mechanically as temperature increases from the glassy state toward the rubbery regime. A preliminary strain-sweep test was performed at 70 °C and 1 Hz to determine the limits of linear viscoelasticity. For both rPET and PEF, the storage modulus remained practically constant at low strain amplitudes, confirming that the samples behave linearly up to strains of about 0.01–0.03 %, depending on the criterion considered. The deformation amplitude for the temperature-ramp experiment was fixed at 0.01% which is inside the linear region.

The temperature-dependent evolution of the storage and loss moduli, respectively noted E′ and E″, was recorded during heating from 70 to 150 °C at 3 °C/min, as shown in Fig.6. For both materials, E′ and E″ decrease sharply when approaching the glass-transition region, reflecting the transition from a glassy to a rubbery state. After the glass transition, rPET shows an increase in both moduli, when the temperature approaches 130 °C. This stiffening is attributed to cold crystallization occurring during heating, as the material reaches its crystallization temperature range. This behavior is consistent with DSC results, which show a clear crystallization peak for PET and rPET. In contrast, PEF does not exhibit any significant increase in moduli over the same temperature range. The storage modulus remains low and changes only slightly with temperature, indicating the absence of crystallization during heating at this rate. This confirms the very slow crystallization kinetics of PEF, in agreement with the DSC measurements, where no crystallization peak is observed under non-isothermal conditions (Fig. 2).

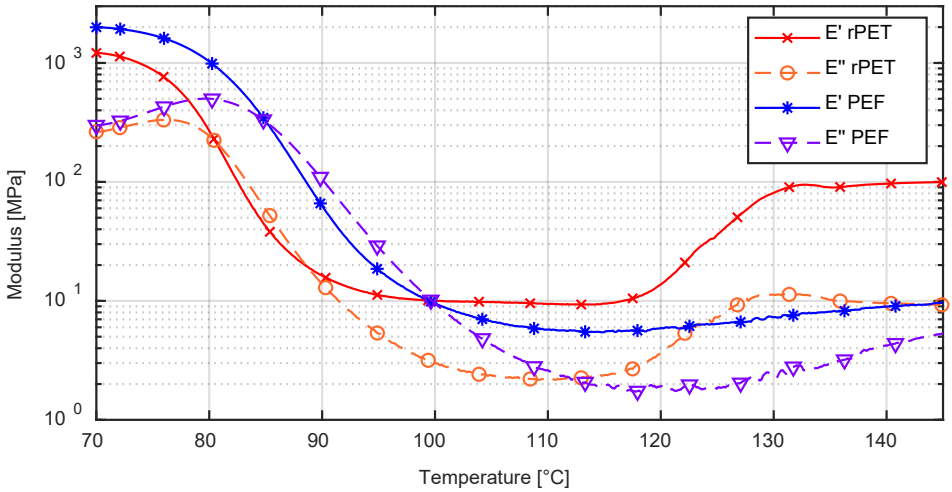

Fig. 6. Evolution of storage and loss moduli for both rPET and PEF

4 Conclusions

This study compared the thermal crystallization behavior of PEF with those of PET and rPET using DSC, optical microscopy and DMA. All analyses were performed on injection-molded plates, representative of the material state before the SBM process. The results highlight clear differences between the materials, particularly in the way PEF crystallizes.

For PET and rPET, the DSC measurements show the expected crystallization and melting peaks, indicating fast crystallization during cooling or isothermal holds. In contrast, PEF does not crystallize under standard non-isothermal DSC conditions. Only long isothermal treatments allow some crystallinity to develop, and the degree of crystallinity remains low. The analysis of X_c as a function of T_i suggests that PEF crystallizes most efficiently between 145 and 160 °C. Consequently, the injected PEF plates are fully amorphous ($X_c \approx 0$). In contrast, the injected PET and rPET plates exhibit a detectable crystalline fraction, with X_c values of about 9%.

Microscopy confirms the strong contrast between PET and PEF. PET forms well-defined spherulites within minutes at 230 °C, whereas no visible crystalline structures appear for PEF under 180 minutes. These images directly illustrate the slower nucleation and growth processes in PEF.
DMA results support the thermal analysis. rPET exhibits a clear increase in both storage and loss moduli when the temperature approaches about 130 °C, which is attributed to cold crystallization during heating. In contrast, PEF shows no comparable stiffening, with moduli remaining low, indicating the absence of crystallization at this heating rate.
Altogether, the results show that PEF behaves very differently from PET or rPET in terms of crystallization. Its very slow thermal crystallization means that it remains essentially amorphous during short processing cycles such as in injection or SBM. This means that crystallization of PEF in such processes is only due to deformation while the crystallization for PET or rPET comes from deformation and heating. These results help clarify how PEF could be integrated into existing PET processing routes and support its potential as a bio-based packaging material.

Appendix: material characteristics

Table A.1 RAMAPET N180 (virgin PET) properties

Property	Unit	Test Method	Typical Value
Intrinsic Viscosity	dL/g	(K) SDP-15 /(R) IND-A-PE-G-IV-01/(Q) CQ-V-1	0.80 ± 0.02
Acetaldehyde	ppm	SDP-21 / IND-A-PE-GC-01 / ASTM F2013	Max 1
Pellet Weight	Pieces/g	SDP-18 / IND-A-PE-PTM-09 / CQ-GA-2	60 ± 5
Fines	Wt%	SDP-60 / IND-A-PE-GA-04 / CQ-GA-4	Max 0.05
Crystalline Density (Solid-stated pellets)	g/cm³	ASTM D1505	1.39 – 1.40
Bulk Density (Poured)	kg/m³	ASTM D1895	830 ± 30
Bulk Density (Vibrated)	kg/m³	ASTM D1895	880 ± 30
Melt Density @ 285 °C	g/cm³	ASTM D1238	1.2
Crystalline Peak Melting Point (Tm)	°C	ASTM D3418	245 ± 5
Glass Transition Temperature (Tg, dry)	°C	ASTM D3418	78 ± 2
Heat of Fusion	kJ/kg	ASTM E793	56 (≈13 cal/g)
Crystallinity (solid-stated pellets)	%	–	50 ± 5%
Pellet Size	mm	–	2.5
Pellet Shape	–	–	Cylindrical
Moisture Content (Pellets)	%	–	< 0.3%

Table A.2 MOPET (rPET) properties

Property	Unit	Test Method	Typical Value
Viscosity (IV)	dL/g	ASTM D1238 / ISO 1133	0.82 – 0.87
Bulk Density	kg/dm³	Internal	0.90 ± 0.50
Melt Filtration	Micron	–	40
Humidity	%	Internal	< 0.4
Pellet Size (M50)	g	Internal	1 ± 0.2
Black Spots (0.5 – 1.0 mm)	%	Internal / DVS AM356	< 10
Black Spots (1.0 – 2.0 mm)	%	Internal / DVS AM356	< 3
Black Spots (> 2.0 mm)	%	Internal / DVS AM356	0
Acetaldehyde	ppm on chip	ASTM 2013	< 1.0
Dust	%	–	< 0.03
Colour L (crystallised)	L	CieLAB	66 – 74
Colour a (crystallised)	a	CieLAB	–4.5 to –1
Colour b (crystallised)	b	CieLAB	–7 to –3

Table A.3 PEF properties

Category	Parameter	Value
General Information	CAS Number	28728-19-0
	Relative Density	1.38
	Molecular Weight	15,000–50,000
Chemical / Physical Properties	Diethylene Glycol (%)	≤ 2
	Inherent Viscosity (dL/g)	0.63–0.85
	Moisture (Wt%)	< 0.8
	Decomposition Temperature (°C)	≥ 350
Mechanical Properties	Tensile Strength (MPa)	70–90
	Elongation at Break (%)	8–25
	Bending Strength (MPa)	110
	Bending Modulus (GPa)	2.2
	Notch Impact Strength (kJ/m²)	2.5
Processing Properties	Melt Index (250 °C)	13–25
Thermal Expansion	Coefficient of Linear Expansion ($°C^{-1}$)	0.002

References

[1] Luan, Q., Li, J., Hu, H., Jiang, X., Zhu, H., Wei, D., Wang, J., & Zhu, J. (2024). Fully Bio-Based 2,5-Furandicarboxylic Acid Polyester toward Plastics with Mechanically Robust, Excellent Gas Barrier and Fast Degradation. ChemSusChem, 17 (14), e202400153. https://doi.org/10.1002/cssc.202400153

[2] Loos, K., Zhang, R., Pereira, I., Agostinho, B., Hu, H., Maniar, D., Sbirrazzuoli, N., Silvestre, A. J. D., Guigo, N., & Sousa, A. F. (2020). A Perspective on PEF Synthesis, Properties, and End-Life. Frontiers in Chemistry, 8, 585. https://doi.org/10.3389/fchem.2020.00585

[3] Forestier, E., Combeaud, C., Guigo, N., & Sbirrazzuoli, N. (2022). A proposal for enhanced microstructural development of Poly(ethylene 2,5-furandicarboxylate), PEF, upon stretching: On strain-induced crystallization and amorphous phase stability improvement. Polymer, 246, 124775. https://doi.org/10.1016/j.polymer.2022.124775

[4] Lightfoot, J. C., Buchard, A., Castro-Dominguez, B., & Parker, S. C. (2022). Comparative Study of Oxygen Diffusion in Polyethylene Terephthalate and Polyethylene Furanoate Using Molecular Modeling: Computational Insights into the Mechanism for Gas Transport in Bulk Polymer Systems. Macromolecules, 55(2), 498–510. https://doi.org/10.1021/acs.macromol.1c01316

[5] Poulopoulou, N., Smyrnioti, D., Nikolaidis, G. N., Tsitsimaka, I., Christodoulou, E., Bikiaris, D. N., Charitopoulou, M. A., Achilias, D. S., Kapnisti, M., & Papageorgiou, G. Z. (2020). Sustainable Plastics from Biomass: Blends of Polyesters Based on 2,5-Furandicarboxylic Acid. Polymers, 12(1), 225. https://doi.org/10.3390/polym12010225

[6] Sousa, A. F., Patrício, R., Terzopoulou, Z., Bikiaris, D. N., Stern, T., Wenger, J., Loos, K., Lotti, N., Siracusa, V., Szymczyk, A., Paszkiewicz, S., Triantafyllidis, K. S., Zamboulis, A., Nikolic, M. S., Spasojevic, P., Thiyagarajan, S., Van Es, D. S., & Guigo, N. (2021). Recommendations for replacing PET on packaging, fiber, and film materials with biobased counterparts. Green Chemistry, 23(22), 8795–8820. https://doi.org/10.1039/D1GC02082J

[7] Luo, Y.-M., Chevalier, L., Monteiro, E., & Utheza, F. (2021). Numerical simulation of self heating during stretch blow moulding of PET: Viscohyperelastic modelling versus experimental results. International Journal of Material Forming, 14(4), 703–714. https://doi.org/10.1007/s12289-020-01565-w

[8] Nguyen, T. T., Luo, Y.-M., Chevalier, L., Baron, A., Lesueur, F., & Utheza, F. (2023). Numerical Simulation of Infrared Heating and Ventilation before Stretch Blow Molding of PET Bottles. International Journal of Material Forming, 16(4), 37. https://doi.org/10.1007/s12289-023-01763-2

[9] Forestier, E., Combeaud, C., Guigo, N., & Sbirrazzuoli, N. (2023). Mechanical Behaviour and Induced Microstructural Development upon Simultaneous and Balanced Biaxial Stretching of Poly(ethylene furandicarboxylate), PEF. Polymers, 15(3), 661. https://doi.org/10.3390/polym15030661

[10] Kasmi, N., Papageorgiou, G. Z., Achilias, D. S., & Bikiaris, D. N. (2018). Solid-State Polymerization of Poly(Ethylene Furanoate) Biobased Polyester, II: An Efficient and Facile Method to Synthesize High Molecular Weight Polyester Appropriate for Food Packaging Applications. Polymers, 10(5), 471. https://doi.org/10.3390/polym10050471

[11] Ioannidis, R. O., Xanthopoulou, E., Terzopoulou, Z., Zamboulis, A., Bikiaris, D. N., & Papageorgiou, G. Z. (2024). Synthesis and thermal investigation of poly(propylene terephthalate-co-2,5-furan dicarboxylate) copolyesters. Journal of Industrial and Engineering Chemistry, 131, 531–544. https://doi.org/10.1016/j.jiec.2023.10.058

[12] Su, K., Luo, W., Xiao, B., Weng, Y., & Zhang, C. (2025). Advancements in the crystallization and regulation of Poly(ethylene 2,5-furandicarboxylate) (PEF): A review. Industrial Crops and Products, 223, 120184. https://doi.org/10.1016/j.indcrop.2024.120184

[13] Papageorgiou, G. Z., Tsanaktsis, V., & Bikiaris, D. N. (2014). Synthesis of poly(ethylene furandicarboxylate) polyester using monomers derived from renewable resources: Thermal behavior comparison with PET and PEN. Phys. Chem. Chem. Phys., 16(17), 7946–7958. https://doi.org/10.1039/C4CP00518J

[14] Luo, Y., Tantchou Yakam, G., Charlot, R., Chevalier, L., & Savajano, R. (2023). In situ adjustment of a visco hyper elastic model for stretch blow molding process simulation of poly-ethylene terephthalate bottles. Polymer Engineering & Science, 63(9), 3066–3082. https://doi.org/10.1002/pen.26428

[15] Nguyen, T., Luo, Y., Chevalier, L., & Jacquet, B. (2025). Impact of the proportion between virgin and recycled polyethylene terephthalate (rPET) on induced microstructure and mechanical stiffness. Polymer Engineering & Science, 65(2), 816-833. https://doi.org/10.1002/pen.27044

[16] Luo, Y.-M., Detrez, F., Chevalier, L., Lu, X., & Roland, S. (2023). Multiscale framework for estimation of elastic properties of Poly ethylene terephthalate from the crystallization temperature. Mechanics of Materials, 181, 104617. https://doi.org/10.1016/j.mechmat.2023.104617

[17] Lauritzen, J. I., & Hoffman, J. D. (1960). Theory of formation of polymer crystals with folded chains in dilute solution. Journal of Research of the National Bureau of Standards Section A: Physics and Chemistry, 64A(1), 73. https://doi.org/10.6028/jres.064A.007

[18] Hoffman, J. D., Weeks, J. J., & Murphey, W. M. (1959). Experimental and theoretical study of kinetics of bulk crystallization in poly(chlorotrifluoroethylene). Journal of Research of the National Bureau of Standards Section A: Physics and Chemistry, 63A(1), 67. https://doi.org/10.6028/jres.063A.005